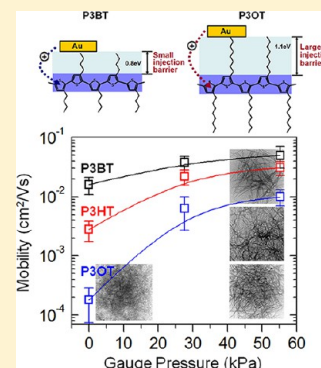


Alkyl Side Chain Length Modulates the Electronic Structure and Electrical Characteristics of Poly(3-alkylthiophene) Thin Films

Hwa Sung Lee,[†] Jeong Ho Cho,[‡] Kilwon Cho,^{§,*} and Yeong Don Park^{||,*}[†]Department of Chemical & Biological Engineering, Hanbat National University, 125, Dongseodaero, Yuseong-gu, Daejeon, 305-719, Republic of South Korea[‡]SKKU Advanced Institute of Nanotechnology (SAINT) and Center for Human Interface Nano Technology (HINT), School of Chemical Engineering, Sungkyunkwan University, Suwon 440-746, Republic of South Korea[§]Department of Chemical Engineering, Pohang University of Science and Technology, Pohang, 790-784, Republic of South Korea^{||}Department of Energy and Chemical Engineering, Incheon National University, Incheon 406-772, Republic of South Korea

S Supporting Information

ABSTRACT: The alkyl side chain length in poly(3-alkylthiophene) (P3AT) was found to affect the electrical properties and molecular electronic structures in thin films. The self-assembly and morphology of a P3AT film was easily controlled through the solvent vapor pressure (varied over the range 0–55 kPa) during solidification. Under high solvent vapor pressure conditions, long dense nanowires formed in the P3AT thin films, and the electrical properties of field-effect transistors (FETs) based on these films improved. The enhancement in the electrical properties of FETs based on a P3AT nanowire structure was strongly affected by the alkyl side chain length. Alkyl side chains in the disordered P3AT thin film act as a barrier to charge movement; however, they assist in the self-assembly of P3AT under high solvent vapor pressures via alkyl chain interactions. Sufficiently long alkyl chains in P3AT molecules, however, form an insulating barrier between the conjugated backbone and the Au electrode, thereby preventing carrier injection and reducing the electrical characteristics of an FET device.



■ INTRODUCTION

Conjugated polymers have attracted considerable attention in the field of organic electronics for their utility in organic light-emitting diodes,¹ organic photovoltaics,^{2–5} and organic field-effect transistors^{6–10} (OFETs). The presence of side chains in a semiconducting molecule makes them solution processable, which facilitates the printing of electronics on a flexible substrate. However, for alkyl side chains, the field-effect mobility is expected to decrease with increasing chain length due to the isolated nature of the alkyl substituents. Several groups have examined the effect of side chains on thin film structures and device performance of conjugated polymer: bulky groups inhibit ordering,¹¹ and low side-chain attachment density promotes three-dimensional ordering.¹² Few studies have examined the effects of linear alkyl side chains on molecular ordering among semiconducting molecules. Linear alkyl side chains endow a molecule with strong van der Waals interactions to facilitate crystallization.¹³ Despite extensive experimental and theoretical investigations, the influence of side chains in a semiconducting molecule on the degree of molecular ordering and the electronic structure in a thin film has not been elucidated, and this relationship remains the subject of extensive discussions.

The high field-effect mobility, stability, and solution processability of poly(3-alkylthiophene)s (P3ATs) having alkyl chains at the 3-position of the thiophene have stimulated significant interest in the utilization of these fascinating

polymers as active materials in organic field-effect transistors (OFETs);^{14,15} however, structural defects in the active layer due to poorly organized molecular arrangements have presented a major challenge to the preparation of high-performance devices based on these solution-processed conjugated polymer films. An effective approach to overcoming this drawback involves the development of well-ordered interconnected nanowires that provide good overlap between the π -orbitals of the conjugated organic molecules and enable efficient charge migration.^{16,17} Unlike the solvent-dropping method, spin-coating methods, which can be used to produce large-scale homogeneous films, cannot be used to produce nanowire morphologies with molecularly ordered structures because rapid solvent evaporation during film formation creates kinetically unfavorable conditions for crystal growth.¹⁸ In an effort to produce molecularly well-ordered structures that yield a high electrical performance, researchers have investigated the effects of post-treatment processes, such as thermal or solvent annealing.^{19–22}

Herein, we report the development of a method for easily manipulating the well-ordered nanowire structures of a P3AT thin film prepared using a spin-coating without post-treatments and the effect of alkyl chain length on the hole-injection barrier

Received: January 6, 2013

Revised: April 15, 2013

Published: May 10, 2013

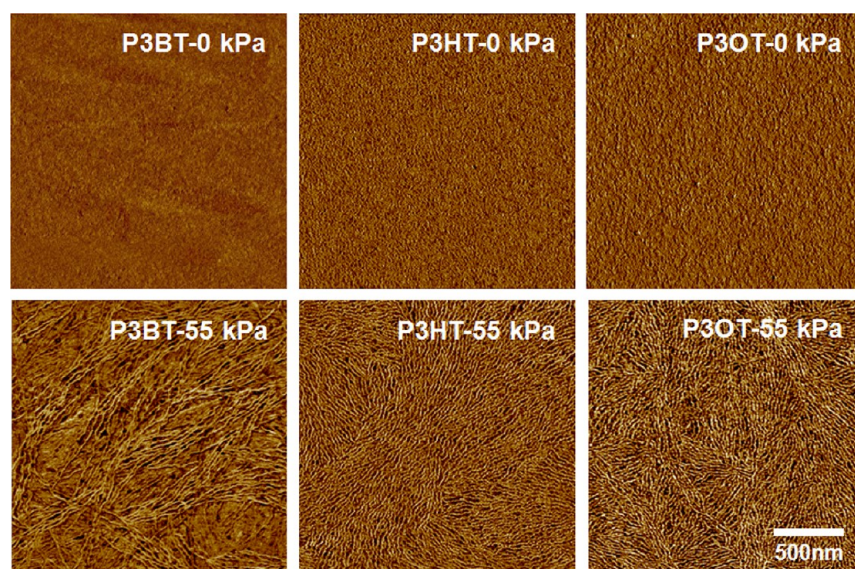


Figure 1. AFM phase images ($2 \times 2 \mu\text{m}^2$) of P3AT films spin-coated under an ambient atmosphere (0 kPa) or under a high solvent vapor pressure (55 kPa).

at the interface between Au and the P3AT thin films. The effects of the solvent vapor pressure on the crystalline and electrical properties of the P3AT film, prepared with various alkyl side chain lengths on the thiophene, are discussed. We systematically investigated the role of the alkyl side chain in the P3AT thin film formed in the presence of a nonzero solvent vapor pressure. We determined the electronic structure of the interface between Au and P3AT (for polymers with different alkyl chain lengths) by means of a low-coverage evaporation technique and synchrotron radiation photoelectron spectroscopy. The differences in the alkyl chain lengths of P3AT provide an excellent opportunity for examining the basic issues involved in the formation of interfaces between metal electrodes and spin-coated polymer semiconductors.

■ EXPERIMENTAL SECTION

Sample Preparation. The P3ATs used in this study, namely, poly(3-butylthiophene) (P3BT), poly(3-hexylthiophene) (P3HT), and poly(3-octylthiophene) (P3OT), were obtained from Rieke Metals Inc. The molecular weights of all alkylthiophenes were similar ($M_n = 20\text{--}25 \text{ kg/mol}$). The spin-coater was placed in a closed chamber fitted with a pressure gauge and a heating plate (Scheme S1 of the Supporting Information, SI). The solvent vapor pressure was readily controlled by increasing the amount of solvent added to the chamber and by modulating the temperature of the chamber. P3AT thin films were spin-coated from 0.75 mg/mL chloroform solutions at 1000 rpm under various solvent vapor pressures. The nanowire shape was precisely observed by transmission electron microscopy (TEM) analysis of the P3AT films, which had been spin-coated from 0.05 mg/mL chloroform solutions under various solvent vapor pressures on a silicon nitride window.

The field-effect mobilities in the P3AT films (P3BT, P3HT, and P3OT) were measured using a top-contact transistor geometry. A 300 nm thick silicon oxide gate dielectric (capacitance = 10.8 nF cm^{-2}) was thermally grown on a highly doped silicon wafer. P3AT chloroform solutions (0.75 mg/mL) were spin-coated at 1000 rpm under various solvent vapor pressures. Finally 150 nm Au source and drain electrodes

were evaporated onto the P3AT thin film surface through a shadow mask, with a channel width of $400 \mu\text{m}$ and a length of $80 \mu\text{m}$.

Characterization. The morphologies of the P3AT nanowires were characterized by TEM (HITACHI-7600), with images collected at 120 kV, and atomic force microscopy (AFM, Digital Instruments Multimode), with images collected in the tapping mode. Grazing-incidence X-ray diffraction (GIXD) measurements were performed on the 3D and 8D beamlines at the Pohang Accelerator Laboratory (PAL) in Korea. The characteristics of the OFETs were obtained at room temperature under ambient conditions using Keithley 2400 and 236 source/measure units.

The electronic structures were analyzed by depositing gold onto the P3AT substrates in several steps (at submonolayer coverages) using an ultrahigh vacuum system (base pressure $<1 \times 10^{-9}$ Torr). The interface between the Au and P3AT was characterized after each step by measuring the valence band spectrum and the secondary electron cutoff by means of synchrotron radiation photoelectron spectroscopy at the 4D and 8A2 beamlines of the PAL in Korea. The gold coverage was determined at each step using a thickness monitor.

■ RESULTS AND DISCUSSION

One of the key steps in the fabrication of P3AT nanowires was the addition of a solvent to the modified spin-coating chamber. This step controlled the solvent vapor pressure, which in turn controlled the solvent evaporation rate from the P3AT solution during solidification. The solvent vapor pressure (0–55 kPa) was tuned by varying the amount of chloroform present in the chamber and the temperature of the spin-coating chamber. The morphological transition of a P3AT thin film, from a featureless thin film to a nanowire film, was characterized by AFM and TEM.

Samples fabricated under ambient conditions (a solvent vapor pressure of 0 kPa) displayed only featureless morphologies, as shown in the AFM (Figure 1) and TEM (Figure 2a) images. As the solvent vapor pressure increased, additional nanowires gradually appeared (Figure S1 of the SI). Samples prepared under high solvent vapor pressures (55 kPa),

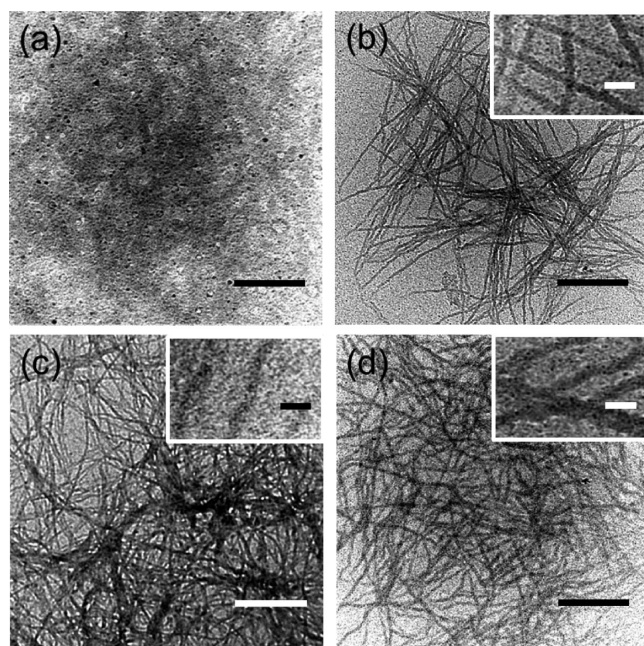


Figure 2. TEM images of spin-coated P3AT films obtained under an ambient atmosphere or under a high solvent vapor pressure: (a) P3HT at 0 kPa, (b) P3BT, (c) P3HT, and (d) P3OT at 55 kPa. (The scale bars for the TEM images and the insets are 500 and 50 nm, respectively.)

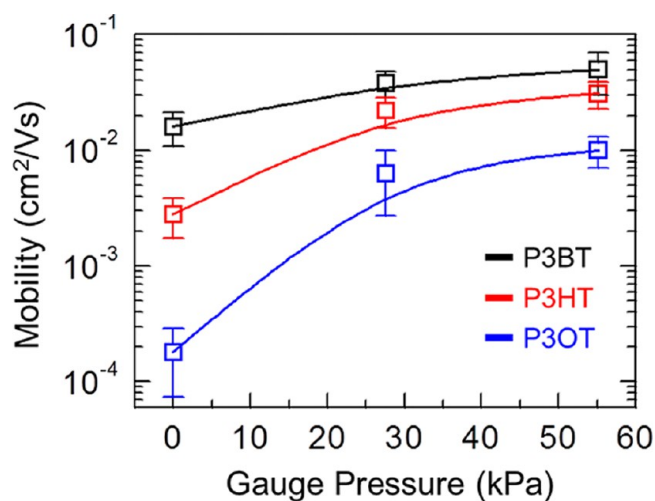


Figure 3. Field-effect mobilities obtained in the saturation regime in P3AT FETs as a function of the solvent vapor pressure.

produced a 1D nanowire network structure in which the nanowires displayed a substantially high aspect ratio. It is possible to infer, therefore, that the solvent vapor assisted the formation of nanowire structures. The high solvent vapor pressure apparently prevented rapid evaporation of the solvent from the P3AT solution, thereby facilitating 1D self-assembly via π - π stacking interaction among the P3AT units during solidification.²³

The P3AT nanowires were characterized by TEM to determine the physical dimensions with greater accuracy than was possible using AFM measurements. Figure 2 shows TEM images, in which the individual nanowire shapes and internal structures are precisely determined in a sample prepared by spin-coating a dilute P3AT chloroform solution (0.05 mg/mL)

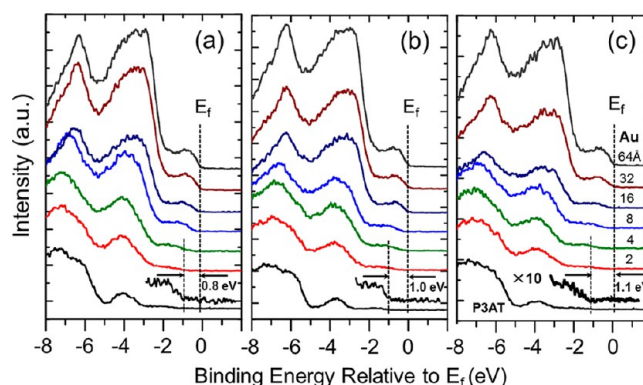


Figure 4. X-ray photoelectron spectra of Au deposited on a P3AT film. Changes in the valence band spectra of the (a) P3BT, (b) P3HT, and (c) P3OT films as a result of Au deposition.

under a nonzero solvent vapor pressure onto a silicon nitride window, which exhibited a surface energy similar to that of the insulator (SiOx) substrate. The TEM images revealed the formation of a network composed of very long fibers with a typical width of 25–40 nm and a length of several micrometers. The inset shows that the width of the P3AT nanowires increased with the alkyl chain length. The TEM and AFM data indicated an increase in the nanowire network structure of the material as a result of controlled aggregation during the spin-casting process.

OFETs with a top-contact geometry were prepared and the charge carrier mobilities were measured to characterize the effects of the P3AT (P3BT, P3HT, and P3OT) morphological features on the electrical properties of the films. Typical drain current vs drain voltage plots at five different gate voltages (V_G) as a function of solvent vapor pressure are shown in Figure S2 of the SI. A clear progression to higher currents is observed. The saturation current reaches a value of $-0.91 \mu\text{A}$ at $V_G = -80$ V for FETs based on P3HT films spin-coated under an ambient atmosphere. Under a high solvent vapor pressure (55 kPa), the saturation current at $V_G = -80$ V increases to $-9.3 \mu\text{A}$. More details can be obtained from the transfer characteristics in Figure S3 of the SI. Figure 3 shows the field-effect mobilities, obtained by plotting the square root of the drain current vs gate voltage ($V_D = -60$ V), as a function of the solvent vapor pressure.²⁴ The P3BT thin film fabricated under a high solvent vapor pressure (55 kPa) yielded a field-effect mobility ($5.0 \times 10^{-2} \text{ cm}^2 \text{V}^{-1} \text{s}^{-1}$) that was only three times the mobility ($1.6 \times 10^{-2} \text{ cm}^2 \text{V}^{-1} \text{s}^{-1}$) of a film prepared under ambient conditions (0 kPa). P3HT thin films fabricated under a high solvent vapor pressure produced a field-effect mobility ($3.0 \times 10^{-2} \text{ cm}^2 \text{V}^{-1} \text{s}^{-1}$) that was more than 1 order of magnitude higher than the mobility of a sample ($2.8 \times 10^{-3} \text{ cm}^2 \text{V}^{-1} \text{s}^{-1}$) prepared under ambient conditions (0 kPa). These surprising enhancements in the field-effect mobility were attributed to the formation of a well-ordered nanowire network morphology under higher solvent vapor pressures, as observed in Figures 1 and 2. This interconnected nanowire network ensured that the conducting channels maintained the connectivity between the source and drain electrodes. The well-ordered structures of the 1D nanowires enabled charge carrier transport across a two-dimensional conjugated network formed by π - π overlap, resulting in a high field-effect mobility.^{25,26}

The field-effect mobility of a P3OT thin film prepared under a high solvent vapor pressure was more than 50 times the

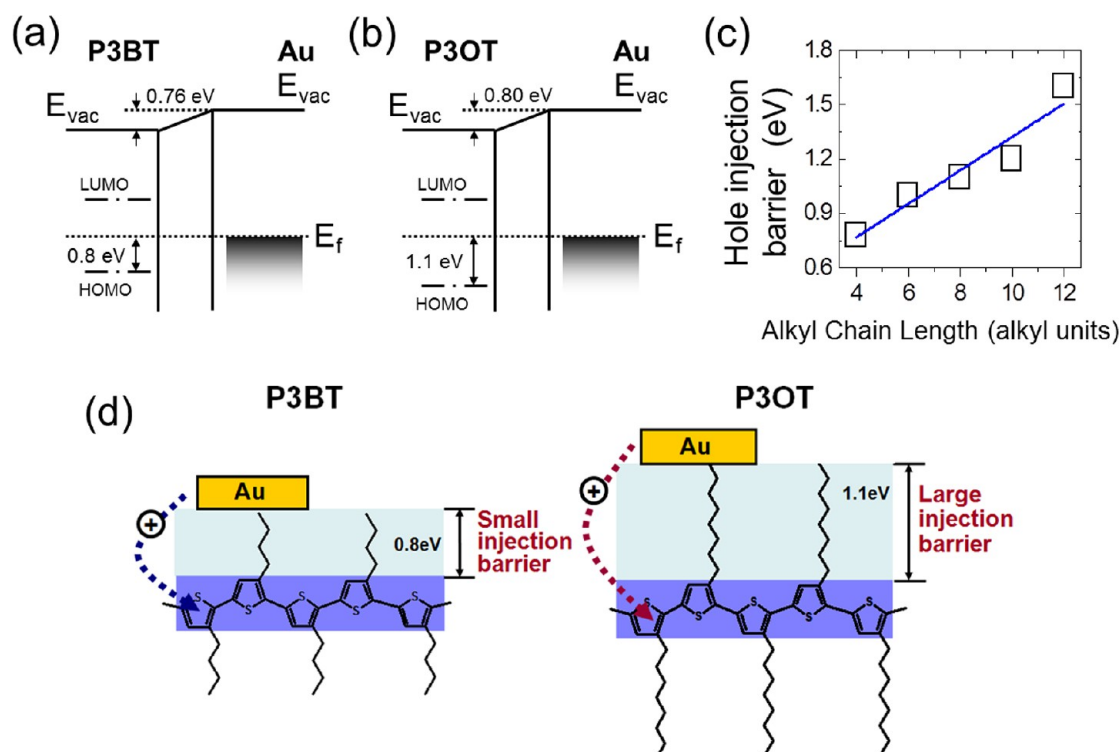


Figure 5. Schematic energy level diagrams of the interfaces between (a) P3BT and Au, and (b) P3OT and Au. (c) The magnitude of the hole-injection barrier from Au to P3AT as a function of the P3AT alkyl side chain length. (d) Schematic representation of hole injection at the interfaces between P3BT and Au (left), and P3OT and Au (right).

mobility obtained from a film prepared under ambient conditions. The pronounced vapor pressure effects in this case were ascribed to the stronger tendency of the polymer chains to assemble through interactions among the long alkyl chains. The effects of the solvent vapor pressure on the field-effect mobility varied significantly with the alkyl side chain length. The alkyl side chains in the disordered P3AT thin films acted as insulators and interfered with the interchain hopping.²⁷ The insulating regions disrupted the packing order among P3AT chains, which reduced the field-effect mobility. Under a high vapor pressure, however, the P3AT molecules formed a lamellar structure in which π -orbital stacking interactions among the conjugated backbones were separated by regions of alkyl side chains. These structures were nominally oriented edge-on, with the π -stacking interactions aligned along the plane of the substrate (Figure S4 of the SI). In the well-ordered P3AT thin film, the side chain ordering improved with the alkyl side chain length. The packing structure among alkyl chains attached to the P3AT backbone changed from a less-ordered configuration to a trans zigzag conformation as the alkyl side chains increased in length.²⁸ Longer alkyl side chains at the 3-position in P3ATs enhanced the side chain ordering.²⁹ Longer branched alkyl side chains and greater alkyl chain separation within a polymer improved the crystalline structures, which improved even further under a high solvent vapor pressure. We concluded that long alkyl side chains in P3OT assisted the self-assembly process in the film under high solvent vapor pressures due to van der Waals interactions among the alkyl chains. The high molecular ordering improved the charge mobility by a factor 50.

Note that P3OT films displayed a lower electrical mobility than the other P3AT films. The injection barrier between the conjugated backbone and the Au electrode was investigated by

characterizing the electronic structures of the interfaces between P3AT and Au, in the P3AT thin films comprising nanowire structures, by synchrotron photoelectron spectroscopy. Figure 4 shows the valence band maxima obtained after Au deposition on the P3BT, P3HT, and P3OT films. Figure 4 shows the changes in the valence band spectra of the Au/P3BT, Au/P3HT, and Au/P3OT systems as a function of the thickness of the deposited Au films. The spectra were recorded using a photon energy of 80 eV. The spectra obtained from P3AT/Si prior to Au deposition yielded the highest occupied molecular orbital (HOMO) levels for the polymers of 0.8 eV (P3BT), 1.0 eV (P3HT), and 1.1 eV (P3OT). As the thickness of the Au layer increased, the HOMO level shifted toward the Fermi level. In other words, the top of the HOMO was 0.8 eV below the Fermi level for P3BT, and 1.1 eV below the Fermi level for P3OT. In this analysis, we assumed that the gap between the HOMO and Fermi levels was the hole-injection barrier, which was smaller for P3BT (with a short alkyl chain length) than for P3OT. We also observed a spectral shift in the P3AT films toward higher binding energies as the length of the alkyl side chains increased [$-(CH_2)_nCH_3$, $n = 3, 5, 7, 9, 11$] (Figures S5 of the SI). In other words, the distance between the Fermi and HOMO levels increased linearly with the alkyl chain length. X-ray photoelectron spectroscopy (XPS) studies showed no changes in the C 1s and S 2p peaks upon Au deposition onto the P3ATs films, indicating that no chemical reaction occurred between Au and P3AT (data not shown).

A schematic energy-level diagram of the interface electronic structure is shown in Figure 5, parts a and b. This diagram shows the values for the interface-dipole (i.e., the vacuum-level offset, obtained from the shift in the secondary electron cutoff) and the hole-injection barrier (obtained from the shift in the valence band maximum after Au deposition onto P3BT and

P3OT). The P3AT thin films prepared with different alkyl chain lengths displayed distinct characteristics. The hole-injection barrier of poly(3-dodecylthiophene), P3DDT (i.e., 1.6 eV), which had a long alkyl chain, was twice that of P3BT (i.e., 0.8 eV), which had a short alkyl chain. The key result is that the hole-injection barrier measured in the edge-on structured P3AT films increased significantly with the alkyl chain length due to an increase in the ionization potential of P3AT (Figure 5c).^{30,31} The magnitude of the interface dipole was relatively independent of the alkyl chain length, whereas the position of the HOMO level relative to the Fermi level shifted downward as the alkyl chain length increased. This observation resulted from the higher ionization potential in the P3ATs prepared with longer alkyl chains. P3OT was expected to form a significantly higher barrier between the conjugated backbone and the Au electrodes, thereby efficiently preventing carrier injection (Figure 5d). For this reason, our study of P3OT-based FETs reports a lower field-effect mobility, even though the mobility was significantly enhanced by the presence of strong alkyl side chain interactions (P3OT is the polymer with the longest alkyl side chains among the P3ATs studied here).

In conclusion, we report a systematic study of the effects of the alkyl side chain length on the electrical characteristics and electronic structures of P3AT. Long alkyl side chains in the P3AT molecules facilitated solution processing by increasing the P3AT solubility and enabling the fabrication of FETs; however, the long alkyl chains also reduced the device performance by forming insulating barrier to charge movement; however, under high vapor pressures, the alkyl side chains in P3AT assisted self-assembly during solidification due to the strong van der Waals interactions among the alkyl chains. P3OT, prepared with long alkyl chains, was found to form a significantly larger barrier between the conjugated backbone and the Au electrode. This barrier efficiently prevented carrier injection and yielded an electrical mobility that was lower than the mobility observed in P3BT films prepared with a short alkyl chain. These results point to the importance of understanding and controlling the molecular design in an organic electronic component. These results may stimulate further studies of the side chain length-dependent on electronic structure and charge carrier transport in other side chain-substituted π -conjugated polymers.

■ ASSOCIATED CONTENT

■ Supporting Information

Schematic representation of the modified spin-coater, AFM images of P3BT films prepared under various solvent vapor pressures, output, and transfer characteristics of the FETs based on P3AT films spin-coated under various solvent vapor pressures, GIXD patterns for P3BT thin films, and the valence band spectra of the P3DT and P3DDT films. This material is available free of charge via the Internet at <http://pubs.acs.org>.

■ AUTHOR INFORMATION

Corresponding Author

*Tel: +82-32-835-8679; e-mail: kwcho@postech.ac.kr (K.C.); ydpark@incheon.ac.kr (Y.D.P.).

Author Contributions

[†]H.S.L. and J.H.C. contributed equally to this work.

Notes

The authors declare no competing financial interest.

■ ACKNOWLEDGMENTS

This research was supported by the Incheon National University Research Grant in 2012 and by Basic Science Research Program through the National Research Foundation of Korea (NRF) funded by the Ministry of Education, Science and Technology (2012R1A1A1004279).

■ REFERENCES

- (1) Burroughes, J. H.; Bradley, D. D. C.; Brown, A. R.; Marks, R. N.; Mackay, K.; Friend, R. H.; Burns, P. L.; Holmes, A. B. Light-Emitting Diodes Based on Conjugated Polymers. *Nature* **1990**, *347*, 539–541.
- (2) Scharber, M. C.; Mühlbacher, D.; Koppe, M.; Denk, P.; Waldauf, C.; Heeger, A. J.; Brabec, C. J. Design Rules for Donors in Bulk-Heterojunction Solar Cells-Towards 10% Energy-Conversion Efficiency. *Adv. Mater.* **2006**, *18*, 789–794.
- (3) Peet, J.; Heeger, A. J.; Bazan, G. C. “Plastic” Solar Cells: Self-Assembly of Bulk Heterojunction Nanomaterials by Spontaneous Phase Separation. *Acc. Chem. Res.* **2009**, *42*, 1700–1708.
- (4) Blom, P. W. M.; Mihailetschi, V. D.; Koster, L. J. A.; Markov, D. E. Device Physics of Polymer:Fullerene Bulk Heterojunction Solar Cells. *Adv. Mater.* **2007**, *19*, 1551–1566.
- (5) Kippelen, B.; Brédas, J. L. Organic Photovoltaics. *Energy Environ. Sci.* **2009**, *2*, 251–261.
- (6) Facchetti, A.; Yoon, M. H.; Marks, T. J. Gate Dielectrics for Organic Field-Effect Transistors: New Opportunities for Organic Electronics. *Adv. Mater.* **2005**, *17*, 1705–1725.
- (7) Lim, J. A.; Liu, F.; Ferdous, S.; Muthukumar, M.; Briseno, A. L. Polymer Semiconductor Crystals. *Mater. Today* **2010**, *13*, 14–24.
- (8) Kline, R. J.; McGehee, M. D. Morphology and Charge Transport in Conjugated Polymers. *Polym. Rev.* **2006**, *46*, 27–45.
- (9) Thompson, B. C.; Fréchet, J. M. J. Polymer–Fullerene Composite Solar Cells. *Angew. Chem., Int. Ed.* **2008**, *47*, 58–77.
- (10) Salleo, A. Charge Transport in Polymeric Transistors. *Mater. Today* **2007**, *10*, 38–45.
- (11) Bao, Z.; Lovinger, A. Soluble Regioregular Polythiophene Derivatives as Semiconducting Materials for Field-Effect Transistors. *Chem. Mater.* **1999**, *11*, 2607–2612.
- (12) Kline, R. J.; DeLongchamp, D. M.; Fischer, D. A.; Lin, E. K.; Richter, L. J.; Chabinyc, M. L.; Toney, M. F.; Heeney, M.; McCulloch, I. Critical Role of Side-Chain Attachment Density on the Order and Device Performance of Polythiophenes. *Macromolecules* **2007**, *40*, 7960–7965.
- (13) Lee, J. S.; Son, S. K.; Song, S.; Kim, H.; Lee, D. R.; Kim, K.; Ko, M. J.; Choi, D. H.; Kim, B. S.; Cho, J. H. Importance of Solubilizing Group and Backbone Planarity in Low Band Gap Polymers for High Performance Ambipolar Field-Effect Transistors. *Chem. Mater.* **2012**, *24*, 1316–1323.
- (14) Arias, A. C.; Endicott, F.; Street, R. A. Surface-Induced Self-Encapsulation of Polymer Thin-Film Transistors. *Adv. Mater.* **2006**, *18*, 2900–2904.
- (15) Park, Y. D.; Lim, J. A.; Lee, H. S.; Cho, K. Interface Engineering in Organic Transistors. *Mater. Today* **2007**, *10*, 46–54.
- (16) Park, Y. D.; Lee, S. G.; Lee, H. S.; Kwak, D.; Lee, D. H.; Cho, K. Solubility-Driven Polythiophene Nanowires and Their Electrical Characteristics. *J. Mater. Chem.* **2011**, *21*, 2338–2343.
- (17) Yang, H.; LeFevre, S. W.; Ryu, C. Y.; Bao, Z. Solubility-Driven Thin Film Structures of Regioregular Poly(3-hexyl thiophene) Using Volatile Solvents. *Appl. Phys. Lett.* **2007**, *90*, 172116–1–172116–3.
- (18) Liu, J.; Sheina, E. E.; Kowalewski, T.; McCullough, R. D. Tuning the Electrical Conductivity and Self-Assembly of Regioregular Polythiophene by Block Copolymerization: Nanowire Morphologies in New Di- and Triblock Copolymers. *Angew. Chem., Int. Ed. Engl.* **2002**, *41*, 329–332.
- (19) Zen, A.; Pflaum, J.; Hirschmann, S.; Zhuang, W.; Jaiser, F.; Asawapirom, U.; Rabe, J. P.; Scherf, U.; Neher, D. Effect of Molecular Weight and Annealing of Poly(3-hexylthiophene)s on the Performance of Organic Field-Effect Transistors. *Adv. Funct. Mater.* **2004**, *14*, 757–764.

- (20) Jo, J.; Kim, S.-S.; Na, S.-I.; Yu, B.-K.; Kim, D.-Y. Time-Dependent Morphology Evolution by Annealing Processes on Polymer:Fullerene Blend Solar Cells. *Adv. Funct. Mater.* **2009**, *19*, 866–874.
- (21) Li, G.; Yao, Y.; Yang, H.; Shrotriya, V.; Yang, G.; Yang, Y. “Solvent Annealing” Effect in Polymer Solar Cells Based on Poly(3-hexylthiophene) and Methanofullerenes. *Adv. Funct. Mater.* **2007**, *17*, 1636–1644.
- (22) Di, C.; Lu, K.; Zhang, L.; Liu, Y.; Guo, Y.; Sun, X.; Wen, Y.; Yu, G.; Zhu, D. Solvent-Assisted Re-annealing of Polymer Films for Solution-Processable Organic Field-Effect Transistors. *Adv. Mater.* **2010**, *22*, 1273–1277.
- (23) Kim, D. H.; Jang, Y.; Park, Y. D.; Cho, K. Controlled One-Dimensional Nanostructures in Poly(3-hexylthiophene) Thin Film for High-Performance Organic Field-Effect Transistors. *J. Phys. Chem. B* **2006**, *110*, 15763–15768.
- (24) Horowitz, G. Organic Field-Effect Transistors. *Adv. Mater.* **1998**, *10*, 365–377.
- (25) Sirringhaus, H.; Brown, P. J.; Friend, R. H.; Nielsen, M. M.; Bechgaard, K.; Langeveld-Voss, B. M. W.; Spiering, A. J. H.; Janssen, R. A. J.; Meijer, E. W.; Herwig, P.; de Leeuw, D. M. Two-Dimensional Charge Transport in Self-Organized, High-Mobility Conjugated Polymers. *Nature* **1999**, *401*, 685–688.
- (26) Tsao, H. N.; Cho, D.; Andreasen, J. W.; Rouhanipour, A.; Breiby, D. W.; Pisula, W.; Müllen, K. The Influence of Morphology on High-Performance Polymer Field-Effect Transistors. *Adv. Mater.* **2009**, *21*, 209–212.
- (27) Kaneto, K.; Lim, W. Y.; Takashima, W.; Endo, T.; Rikukawa, M. Alkyl Chain Length Dependence of Field-Effect Mobilities in Regioregular Poly(3-alkylthiophene) Films. *Jpn. J. Appl. Phys.* **2000**, *39*, L872–L874.
- (28) Park, Y. D.; Kim, D. H.; Jang, Y.; Cho, J. H.; Hwang, M.; Lee, H. S.; Lim, J. A.; Cho, K. Effect of Side Chain Length on Molecular Ordering and Field-Effect Mobility in Poly(3-alkylthiophene) Transistors. *Org. Electron.* **2006**, *7*, 514–520.
- (29) Bao, Z.; Dodabalapur, A.; Lovinger, A. Soluble and Processable Regioregular Poly(3-hexylthiophene) for Thin Film Field-Effect Transistor Applications with High Mobility. *Appl. Phys. Lett.* **1996**, *69*, 4108–4110.
- (30) Schulze, K.; Riede, M.; Brier, E.; Reinold, E.; Bäuerle, P.; Leo, K. Dicyanovinyl-Quinqueithiophenes with Varying Alkyl Chain Lengths: Investigation of Their Performance in Organic Devices. *J. Appl. Phys.* **2008**, *104*, 074511–1–074511–5.
- (31) Halik, M.; Klauk, H.; Zschieschang, U.; Schmid, G.; Ponomarenko, S.; Kirchmeyer, S.; Weber, W. Relationship Between Molecular Structure and Electrical Performance of Oligothiophene Organic Thin Film Transistors. *Adv. Mater.* **2003**, *15*, 917–922.